

Available online at [www.sciencedirect.com](http://www.sciencedirect.com)

**jmr&t**  
Journal of Materials Research and Technology  
journal homepage: [www.elsevier.com/locate/jmrt](http://www.elsevier.com/locate/jmrt)



## Original Article

# Numerical study on impact resistance of novel multilevel bionic thin-walled structures

Zhiquan Wei, Xianghong Xu<sup>\*</sup>

LNM, Institute of Mechanics, Chinese Academy of Sciences, Beijing, 100190, China

## ARTICLE INFO

## Article history:

Received 27 October 2021

Accepted 22 December 2021

Available online 28 December 2021

## Keywords:

Bionic structure design

Thin-walled structure

Impact resistance

## ABSTRACT

Inspired by impact-resistant hedgehog spine and beetle's forewing, the thin-walled structures of simple hedgehog spine and multilevel hedgehog spine were designed. Numerical simulations of rigid flat plate impacting on thin-walled structures showed that the deformation coordination ability and stress distribution of the structure are improved effectively by the hedgehog spine section design. This makes the specific energy absorption of the simple hedgehog spine thin-walled structure just before failure increase to 9.6 times and 5.7 times those of the single-walled cylinder and simple spider web thin-walled structures, respectively. Furthermore, the sub-circle multilevel design was introduced to further increase the range of high strain energy density, and the specific energy absorption of the multilevel hedgehog spine thin-walled structure was 2.1 times that of the simple hedgehog spine thin-walled structure.

© 2021 The Author(s). Published by Elsevier B.V. This is an open access article under the CC BY-NC-ND license (<http://creativecommons.org/licenses/by-nc-nd/4.0/>).

## 1. Introduction

Thin-walled structures boasting high specific energy absorption (SEA), i.e., the energy absorbed per unit mass, are commonly used as impact protection devices in fields such as transportation and aerospace [1,2]. Specifically, a typical thin-walled structure can be found in the crush box installed in the front of a vehicle. When a vehicle collision occurs, the energy-absorbing box is the first part to deform, by which energy can be absorbed, so as to effectively avoid the damage to the longitudinal beam of the vehicle body [3,4]. In an aircraft crash, the fuselage bottom is the first part to collide with the ground. The fuselage bottom is made of cross-connected composite plates, which are usually designed as thin-walled structures due to the high energy absorption of its crush

failure [5]. In practical engineering applications, higher impact speed is more likely to cause severe accidents, which may result in economic losses or casualties. Therefore, it is necessary to further increase the impact resistance of thin-walled structures to improve their safety and reliability. Most conventional thin-walled structures are simply single-walled or multi-walled, with cross sections usually shaped as circular, triangular or square ring and wall thickness uniform along the axis. There is no connecting element between walls or themselves. Although these thin-walled structures are easy to prepare and inexpensive, their specific energy absorptions need to be further improved to meet practical demands.

In recent years, researchers have turned to imitating and learning from biological structures to find more effective

<sup>\*</sup> Corresponding author.

E-mail address: [xxh@lnm.imech.ac.cn](mailto:xxh@lnm.imech.ac.cn) (X. Xu).

<https://doi.org/10.1016/j.jmrt.2021.12.105>

2238-7854/© 2021 The Author(s). Published by Elsevier B.V. This is an open access article under the CC BY-NC-ND license (<http://creativecommons.org/licenses/by-nc-nd/4.0/>).

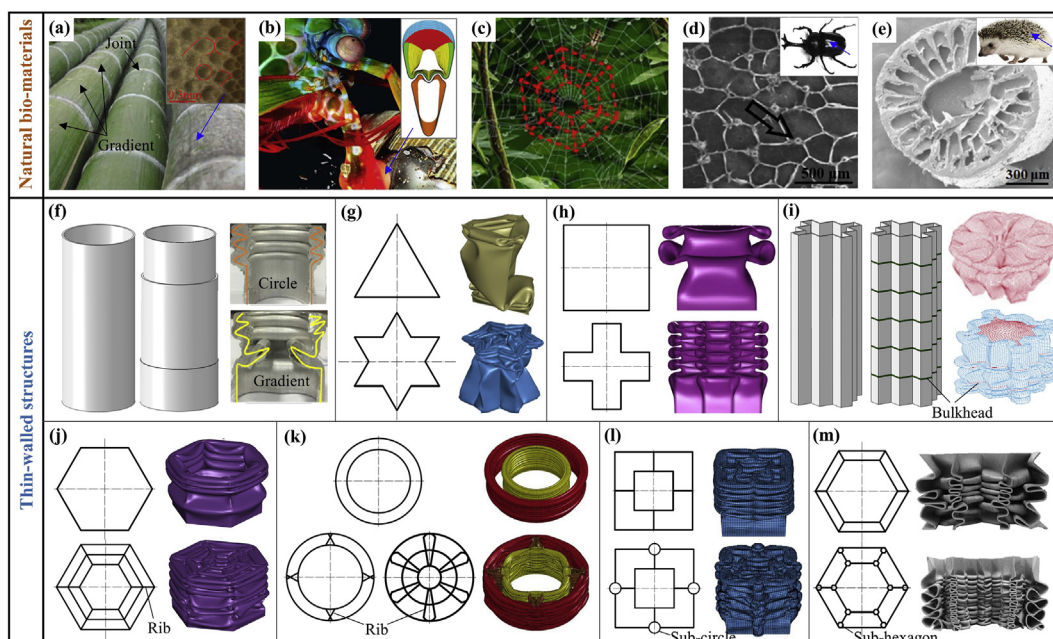


**Fig. 1 – Impact-resistant biological materials in nature and artificial thin-walled structures. Biological materials: (a) Bamboo [9,11]; (b) Mantis shrimp's dactyl club [12]; (c) Spider web [15]; (d) Beetle's forewing [16]; (e) Hedgehog spine [18,19]. Thin-walled structures: (f) Gradient single-walled structure [9]; (g) Star shaped single-walled structure [20]; (h) Criss-cross single-walled structure [21]; (i) Non-convex icosagon shaped single-walled structure with partition plates [10]; (j) Ribbed hexagonal triple-walled structure [15]; (k) Circular multi-walled structures with X-shaped and tapered ribs [11,12]; (l) Ribbed square double-walled structure with hollow cylinders [16]; (m) Ribbed hexagonal double-walled structure with subnormal hexagons [15].**

designs to improve the impact resistance of thin-walled structures. Numerous impact-resistant biological materials/structures so far have been found in nature [6–8]. Their structures and functions have been continuously optimized and improved through billions of years of natural selection and evolution. Bamboo is lightweight and highly efficient energy-absorbing due to its gradient variation in wall thickness and joint spacing along the growth direction, and several kinds of differently shaped rib structures in the cross section (Fig. 1(a)) [9–11]. Mantis shrimp's hammer-shaped dactyl club, with a conical cross-section and two cavities in it (Fig. 1(b)), can easily penetrate shells known for toughness with almost no damage to itself [12–14]. When the spider web, which composed of multiple polygons and ribs (Fig. 1(c)), is subject to a low-speed impact, large deformation occurs in the impacted area and the ribs allow the area away from the impact point deform accordingly, expanding the strain energy storage area and effectively dissipating the impact energy, thus maintaining its structural integrity [15]. Beetle's forewing is a composite sandwich structure, consisting of upper and lower skins and honeycomb-type ribs, with hollow cylinders distributed in the center of the ribs and the joints (Fig. 1(d)). This multilevel structure can reduce the weight of forewing while effectively absorbing the impact energy of external objects such as raindrops, providing a protection for the body [16,17]. A hedgehog spine has 22 ribs extending from bottom to tip in it, which evenly divide the cross-section circumference (Fig. 1(e)). It is mainly attributed to the extremely high shock absorption of spines that a hedgehog can fall from a height of

tens of meters and hit the ground at a speed of 15 m/s, almost uninjured [18,19]. Undoubtedly, the perfect structures of these naturally impact-resistant biomaterials provide useful insights into the design of thin-walled structures.

The single-walled structure is a typical and simple thin-walled structure, which is easy to design and manufacture. By changing the geometry of its axial or transverse section, its energy absorption performance can be further improved. Jia et al. [9] designed a gradient single-walled structure after the gradient variation of bamboo wall thickness and joint spacing along the growth direction, which consists of three segments with length and wall thickness varying along the axial in a gradient mode (Fig. 1(f)). The pendulum impact test and finite element simulation showed that when the thin-walled structure was under axial impact, the circular single-walled structure folded three times, while the gradient single-walled structure folded four times due to the discontinuity of wall thickness, and the number of folds increased during the impact process, resulting in a larger deformation area and more energy absorbed. The SEA of the gradient single-walled structure increased by 6.2% compared with the circular single-walled structure. Based on simpler triangle and square, Wang et al. [20] generated thin-walled structures with cross-sections geometry of star based on simpler triangle (Fig. 1(g)), while Sun et al. [21] and Liu et al. [10] generated thin-walled structures with cross-sections geometry of criss-cross (Fig. 1(h)) and non-convex icosagon (Fig. 1(i)), respectively. The numerical results showed that the deformation tended to be more uniform during the impact process due to the

increased corner restraint. Moreover, compared with the conventional triangular single-walled structure, the maximum impact load and the specific energy absorption for the star shaped single-walled structure were increased by 40% and 100.1%, respectively. And compared with the square single-walled structure, the maximum impact loads for the criss-cross and non-convex icosagon shaped single-walled structures were increased by 25% and 65%, respectively, and the specific energy absorptions were increased by 146.2% and 104.0%, respectively. Synergy between thin walls and partition plates or ribs can be generated by addition of partition plates or ribs to the single/multi-walled structure, to increase the maximum impact load and the strain storage area, by which higher energy absorption can be gained compared with conventional single/multi-walled structures. Liu et al. [10] added partition plates to the non-convex icosagon shaped single-walled structure inspired by bamboo joints (Fig. 1(i)). The results of simulation showed that the partition plates can effectively prevent the transverse expansion of the thin-walled structure under impact and make the thin-walled structure fold steadily. Compared with the non-convex 20-sided single-walled structure without partition plate, the maximum impact load was increased by 42%, the number of folds was increased from 2 to 5, the strain storage area was also increased, and the specific energy absorption was increased by 114.0%. Inspired by spider web, Zhang et al. [15] designed a ribbed hexagonal triple-walled structure based on the conventional hexagonal single-walled structure (Fig. 1(j)). The results of finite element simulation showed that under impact the maximum impact load was increased by 65%, the number of folds was increased from 4 to 6, and the specific energy absorption was increased by 53.8%, compared with the conventional hexagonal single-walled structure. Fu et al. [11] and Huang et al. [12] imitated the ribbed bamboo structure and the mantis shrimp dactyl club by adding X-shaped ribs and tapered ribs between the circular multi-walled structure (Fig. 1(k)), respectively. The results of simulation showed that the maximum impact loads were increased by 34% and 10%, respectively. The multi-walled area connected to the ribs forms multiple corners, the bending deformation of which can contribute to energy dissipation. Compared with the conventional circular multi-walled structure, the introduction of X-shaped and tapered ribs increased the specific energy absorption of the ribbed multi-walled structure by 37.4% and 20.0%, respectively.

With the development of bionic design, impact-resistant bionic structures are increasingly inclined to be combinatorial, i.e., not just imitating a single organism, but incorporating the characteristics of multiple organisms in one, so that the sub-structures in the combinatorial structure can inherit the advantages of the parent structures, thus maximizing the impact resistance of the bionic structure [22,23]. By introducing multilevel designs into the thin-walled structure, researchers can further increase the synergy between the ribs and the inner and outer walls, which increases the maximum impact load and the energy absorption. Zhang et al. [16] performed a second level design based on a ribbed square double-

walled structure (Fig. 1(l)), by reference to the hollow-cylindrical structure in the forewing of a beetle. The results of finite element simulation showed that the highest specific energy absorption was achieved when hollow cylinders were added into the intersections of the outer wall and the ribs. Due to the increase in deformation in the hollow-cylindrical region, the maximum impact load increased by 51% compared with the ribbed double-walled structure without hollow cylinders. The deformation near the hollow cylinders was also increased, resulting in an increase of 30.2% in the specific energy absorption. Zhang et al. [15] performed a second level design based on the ribbed hexagonal double-walled structure (Fig. 1(m)). The results of simulation showed that the highest specific energy absorption was achieved when subnormal hexagons were added into the intersections of the ribs and the inner and outer walls. Compared with the double-walled structure without subnormal hexagons, more folds occurred inside the structure and the specific energy absorption was increased by 71.6%, although the maximum impact load was only increased by 4%. Therefore, the multilevel design may further improve the impact resistance of thin-walled structures.

Besides the specific energy absorption, the impact force was also used to evaluate the impact resistance performance of thin-walled structures [10–12,15,16,21]. For a thin-walled structure, the maximum impact force and the average impact force could be affected by its geometric dimensions. Especially, they would largely increase with the increase of wall thickness [15,16]. Since excessive impact force may cause casualties of passengers, the maximum impact force should be reduced at a low level. The impact force efficiency was defined as the ratio between the average and maximum impact force. For the single-walled structures as mentioned above, the impact force efficiencies of the gradient and criss-cross shaped single-walled structures were 70% [9] and 51% [21], respectively. For the non-convex icosagon shaped single-walled structures, the impact force efficiency was increased from 49% to 81% after adding the partition plates [10]. Compared with the conventional circular multi-walled structure, the X-shaped and tapered ribs also increased the impact force efficiency of the ribbed multi-walled structure from 43% to 45%–50% and 60%, respectively [11,12]. By contrast, the impact force efficiency of multilevel spider web thin-walled structure was largely increased from 50% to 88% by taking the multilevel design [15].

In this paper, a simple hedgehog spine structure was designed by reference to the microstructural characteristics of the impact-resistant hedgehog spine. On this basis, a multilevel hedgehog spine structure was designed by introducing hollow cylinders as the substructure, referring to the impact-resistant forewing of the beetle. By finite element method, the process of rigid flat plate impacting thin-walled structure was simulated. Then, the impact resistances of the conventional single-walled cylindrical structure, simple and multilevel spider web structures with higher energy absorption in existing literature and the simple and multilevel hedgehog structures designed in this paper were compared, and the

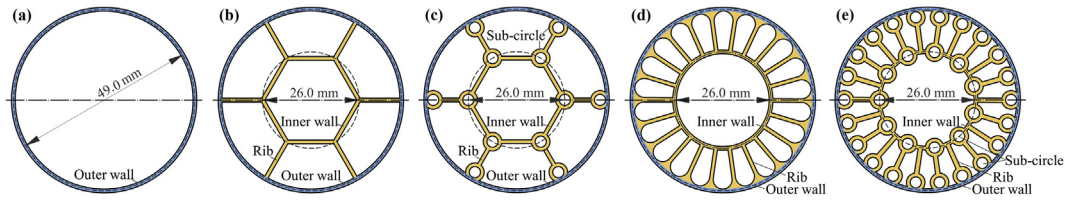


**Fig. 2 – Cross-sections of thin-walled structures. (a) Single-walled cylinder; (b) Simple spider web; (c) Multilevel spider web; (d) Simple hedgehog spine; (e) Multilevel hedgehog spine.**

mechanism was analyzed. Finally, the influence of the number of ribs and the sub-circular radius on the impact resistance of multilevel hedgehog structure was discussed, which provides a reference for the design of new impact-resistant thin-walled structures.

## 2. Finite element modelling of impact process of bionic thin-walled structures

### 2.1. Geometric model

Figure 2 illustrates the cross-sections of thin-walled structures: single-walled cylinder, simple spider web, simple hedgehog spine, multilevel spider web and multilevel hedgehog spine. The latter four thin-walled structures have different internal structures, and their outer walls are a single-walled cylinder (Fig. 2(a)). The internal structures of the simple spider web and simple hedgehog spine structures have 6 ribs (Fig. 2(b)) and 22 ribs (Fig. 2(d)), respectively, the same as the natural spider webs and hedgehog spines. The outer wall of the simple hedgehog spine structure is connected to the ribs by an arc transition that is tangential to both adjacent ribs as well as to the outer wall. Based on the simple spider web structure, a sub-circle is added to the intersection of the center line of each rib and the center lines of the inner and outer walls. A multilevel spider web structure is then generated by keeping the center line of the outer wall tangent to the center line of the sub-circle and the center line of the inner wall intersect with the center of the sub-circle (Fig. 2(c)) [15]. Based on the simple hedgehog spine structure, 22 sub-circles are added at the positions where the ribs are attached to the outer wall and 11 sub-circles are added at the intersections of the ribs and the inner wall center line alternately. A multilevel hedgehog spine structure is then generated by keeping the sub-circle center line on the outer wall tangent to the outer wall center line and the sub-circle center on the inner wall intersect with the inner wall center line (Fig. 2(e)). For the five thin-walled structures, the axial height is 75.0 mm, the diameter of the middle line of the outer wall is 49.0 mm, the diameter of the center line of the inner circle or the circum-circle of the regular hexagon is 26.0 mm, and the thickness of the inner walls, the out walls, and the ribs is 1.0 mm. The radius of the midline of the sub-circle is 2.0 mm, and the thickness of the sub-circle wall is 1.0 mm.

### 2.2. Material parameters

According to the ASTM D638 standard, dumbbell-shaped tensile samples of stiff material Verowhite were prepared with the 3D printing technology, and the gauge length section had a length of 25 mm, a width of 6 mm and a thickness of 3 mm. Single axial tensile tests were performed by using Instron 5848 MicroTester at a tensile speed of 500 mm/min. Then the nominal stress  $\sigma_n$  was obtained by dividing the load output of the testing machine by the measured area  $17.9 \text{ mm}^2$  of the original cross section of a mark section. The surface of the sample subjected to speckle treatment was synchronously shot by using a camera. The deformation of the gauge length section along the stretching direction was calculated by using a digital speckle correlation method, and the nominal strain  $\epsilon_n$  was obtained by dividing the deformation by the measured value 25.0 mm of the original length of the mark section. Further, true stress  $\sigma = \sigma_n(1+\epsilon_n)$  and true strain  $\epsilon = \ln(1+\epsilon_n)$  were calculated [24]. A true stress–strain curve of Verowhite was obtained [22]. Since Verowhite-like materials do not have a significant strain rate effect [25], it was assumed that

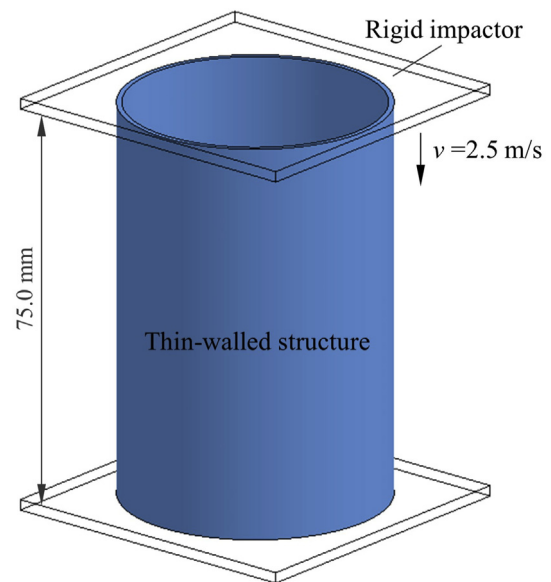


**Fig. 3 – Schematic sketch of a rigid flat plate impacting the thin-walled structure.**

**Table 1 – LS-DYNA parameters used in the finite element simulation.**

Type	Wall thickness (mm)	Meshing				Friction coefficient		Hourglass control type
		Mesh size (mm)	Element number	Node number	Mesh metric	Static	Dynamic	
Single-walled cylinder	12.5	1.20	114,534	122,496	0.90	0.2	0.2	Flanagan-Belytschko stiffness form
	5.3	0.90	110,208	124,525	0.94			
	1.0	0.80	37,788	56,050	0.86			
Simple spider web	1.0	0.85	63,101	94,590	0.85			
Simple hedgehog spine	1.0	0.80	117,030	166,345	0.88			
Multilevel spider web	1.0	0.80	96,444	138,415	0.84			
Multilevel hedgehog spine	1.0	0.80	177,566	246,050	0.81			

material constitutive curves obtained at medium and high strain rates were the same as that obtained at low strain rate. The Verowhite elastic modulus was 3.00 GPa, the Poisson was 0.30, and the density was 1200 kg/m<sup>3</sup> [25].

### 2.3. Finite element simulation

The nonlinear dynamics finite element software LS-DYNA was used to simulate the process of a flat plate impacting the thin-walled structures (Fig. 3). A specific elastic–plastic constitutive model (\*MAT\_PLASTICITY\_POLYMER) [26] for high polymers in LS-DYNA Material Database was adopted for Verowhite. The failure and deletion of an element was simulated by the first principal stress failure criterion (\*MAT\_ADD\_EROSION), which means that, when the first principal stress of a certain element exceeds the failure stress, the element will be deleted. Moreover, the failure stress of Verowhite was 64 MPa. In our previous impact numerical simulation study [22], the constitutive model and related parameters of VeroWhite had been validated by impact experiments. Commercial software Workbench was used for preprocessing and finite element meshing. A structural grid division and hexahedron element were adopted. The meshing size, element and node numbers of the thin-walled structures and thick-walled cylinder were given in Table 1. Their average mesh metric values were greater than 0.8, which indicated they all had good grid quality.

**Table 2 – MIF, SEA, AIF and IFE of thin-walled structures and thick-walled cylinder before failure.**

Type	Wall thickness (mm)	MIF (kN)	SEA (kJ/kg)	AIF (kN)	IFE (%)
Single-walled cylinder	12.5	108.76	24.22	106.19	88.64
	5.3	47.20	4.31	40.17	85.11
	1.0	7.10	0.70	4.85	68.31
Simple spider web	1.0	16.65	1.18	11.62	69.79
Simple hedgehog spine	1.0	36.72	6.69	32.12	87.47
Multilevel spider web	1.0	21.30	1.36	14.90	69.95
Multilevel hedgehog spine	1.0	47.20	13.86	42.21	89.43

The thin-walled structures were modeled with the axial direction perpendicular to the base, the lower end fixed to the base, and the upper end impacted by a 500 kg flat plate with an initial velocity of 2.5 m/s. The flat plate and the support were simplified as rigid bodies (\*MAT\_RIGID). The maximum displacement of the rigid flat plate was set as 30 mm. All degrees of freedom in the non-impact directions of the rigid flat plate were limited. The lower ends of the structures were bound to a fully fixed support restraint. Furthermore, in order to avoid unexpected penetration, eroding single surface contact (\*CONTACT\_ERODING\_SINGLE\_SURFACE) was defined in areas where contact may occur. In addition, the static/dynamic friction coefficient and hourglass control type were given in Table 1.

### 2.4. Impact resistance indicators

To evaluate the impact resistance performance of the thin-walled structures under axial impact, the specific energy absorption (SEA), maximum impact force (MIF), average impact force (AIF) and impact force efficiency (IFE) were considered in this paper, respectively. The SEA was employed to quantify the efficiency of energy absorption per unit mass, where the absorbed energy of structure was calculated by the difference between the initial and final kinetic energies of the rigid flat plate. Generally, the higher the SEA, the better was the energy absorption performance of structure. The AIF was defined as the total absorbed energy of structure divided the corresponding displacement of the rigid flat plate. The MIF should be reduced or constrained to certain extent and 50 kN was chosen as the maximum value in this paper. The IFE indicated the constancy of the impact force during impact, and it was defined as the ratio between the AIF and the MIF. Obviously, the higher the IFE, the better was the impact force uniformity.

## 3. Results and discussion

### 3.1. Impact resistance performance of thin-walled structure

The MIF, SEA, AIF and IFE of the five thin-walled structures before failure were shown in Table 2. Two thick-walled

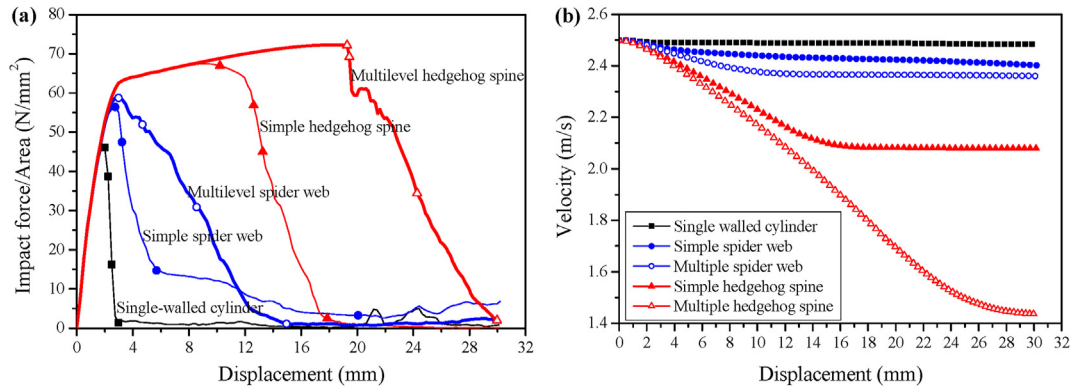


Fig. 4 – (a) Impact force ratio and (b) velocity of rigid flat plate versus axial displacement.

cylinder structures with the wall thickness of 12.5 mm and 5.3 mm were also considered. The former wall thickness meant the cylinder with 50 mm outer diameter and 25 mm inner diameter. The latter wall thickness meant the cylinder with 50 mm outer diameter and 39.4 mm inner diameter. For the same 1.0 mm wall thickness of five thin-walled structures, according to the ascending order of MIF, SEA, AIF and IFE, they were the single-walled cylinder, simple spider web, multilevel spider web, simple hedgehog spine and multilevel hedgehog spine, respectively. The SEAs of the simple spider web and multilevel spider web structures were 1.7 and 1.9 times that of the single-walled cylinder structure, respectively, while the SEAs of the simple hedgehog spine and multilevel hedgehog spine thin-walled structures were 9.6 and 19.8 times that of the single-walled cylinder structure, respectively. Obviously, the SEAs of the simple hedgehog spine and multilevel hedgehog spine thin-walled structures were 5.7 and 10.2 times those of the simple spider web and multilevel spider web structures, respectively. On the other hand, the multilevel structure design has little effect on the SEA of the spider web thin-walled structure, while it doubles the SEA of the hedgehog spine thin-walled structure. The MIFs of simple hedgehog spine and multilevel hedgehog spine structures were both high, but less than 50 kN, within the allowable range. By contrast, the thick-walled cylinder structure with 12.5 mm wall thickness had excellent SEA, but excessive high MIF of 108.76 kN which exceeded the allowed maximum value. The MIF of thick-walled cylinder structure with 5.3 mm wall thickness was same with the multilevel hedgehog spine structure. However, its SEA was only 4.31 kJ/kg, 0.3 times that of the multilevel hedgehog spine structure. Additionally, its IFE was 85.11%, slightly lower than the multilevel hedgehog spine structure 89.43%. The simple hedgehog spine and multilevel hedgehog spine structures had higher IFE about 88% compared with the simple spider web and multilevel spider web structures about 70%.

The five thin-walled structures of single-walled cylinder, simple spider web, simple hedgehog spine, multilevel spider web and multilevel hedgehog spine had equal axial height and relative density. The impact force ratio, i.e., the axial impact force of the rigid flat plate divided by the actual area of the cross-section of a thin-walled structure, was used to represent the impact force per unit area of the thin-walled structure.

Figure 4(a) shows the variation curve of impact force ratio with axial displacement. When the axial displacement does not exceed  $u_L$ , the impact force ratio versus displacement curves of the five thin-walled structures are in a linear stage, and as the displacement increases, the impact force ratio increases approximately linearly. For the single-walled cylinder, simple spider web and multilevel spider web structures, the end displacements  $u_L$  in the linear stage are 2.0 mm, 2.7 mm and 3.0 mm, respectively, and the impact force ratios reach the maximums at this moment; subsequently, elements failure occur and these three structures enter the failure stage. For the simple hedgehog spine and multilevel hedgehog spine structures,  $u_L$  is 3.0 mm; after the linear stage, both structures undergo a yield stage, in which as the displacement increases, the impact force ratio slowly increases and then slightly decreases until the axial displacements reach 10.2 mm and 19.3 mm, respectively; at the next moment, the structures enter the failure stage and experience element failure. Obviously, unlike the former three thin-walled structures, the two hedgehog spine structures have obvious yield stages, and the axial deformation of the multilevel hedgehog spine structure in the yield stage is greater.

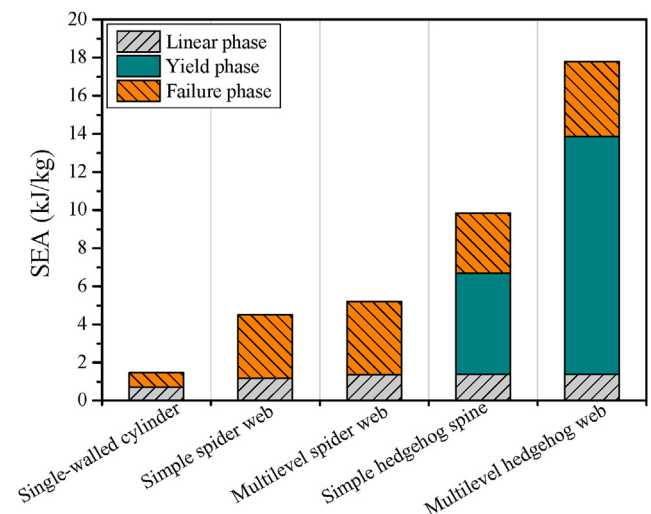
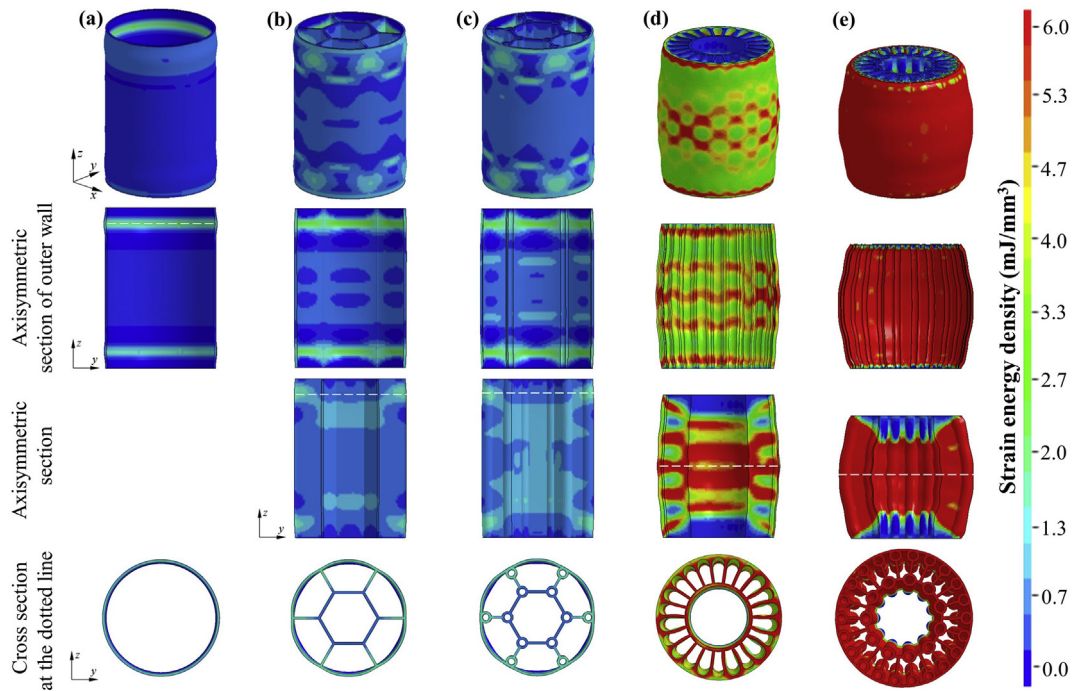


Fig. 5 – Specific energy absorptions of the five thin-walled structures.



**Fig. 6 – Strain energy density fields of the five thin-walled structures at the moment before failure. (a) Single-walled cylinder; (b) Simple spider web; (c) Multilevel spider web; (d) Simple hedgehog spine; (e) Multilevel hedgehog spine.**

Based on the variation curve of the velocity of the rigid flat plate with displacement under impact (Fig. 4(b)), the difference between the initial and final kinetic energies of the rigid plate at a certain stage, i.e., the energy absorbed by the structure at that stage, was calculated, and then divided by the mass of the structure to obtain the SEA. Figure 5 illustrates the SEAs of the five structures in the linear stage, yield stage and failure stage. The end displacements for the five structures in the failure stages were set as 30 mm.

In the linear stage, the SEA of the single-walled cylinder was 0.70 kJ/kg; the SEA of the simple spider web structure was 1.18 kJ/kg, which is 1.7 times that of the single-walled cylinder; the SEAs of the three thin-walled structures of multilevel spider web, simple hedgehog spine and multilevel hedgehog spine were similar, about 1.38 kJ/kg, twice that of the single-walled cylinder. In other words, the cross-sectional designs of spider web and hedgehog spine enhanced the energy absorption performance of the thin-walled structures in the linear stages. In addition, the multilevel structure design slightly improved the SEA of the linear section of the spider web thin-walled structure by about 15%, while it did not improve the energy absorption performance of the hedgehog spine thin-walled structure in the linear stage. Subsequently, the two hedgehog structures underwent a yield deformation stage. In the yield stage, the SEAs of the hedgehog and multilevel hedgehog structures were 5.30 kJ/kg and 12.48 kJ/kg, 3.8 and 9.0 times those of their linear stages, respectively. In other words, both the hedgehog cross-section and the multilevel structure design significantly improved the energy absorption performance of the structure before failure. In the

failure stage, the SEA of the single-walled cylinder was 0.77 kJ/kg; the SEAs of the simple spider web and simple hedgehog spine structures were similar, about 3.23 kJ/kg, 4.2 times that of the single-walled cylinder; the SEAs of the multilevel spider web and multilevel hedgehog spine thin-walled structures were also similar, 3.89 kJ/kg, 5.1 times that of the single-walled cylinder. In other words, the spider web and hedgehog spine cross-sectional design effectively improved the energy absorption performance of the failure stage. In addition, the multilevel structure design slightly improved the SEAs of the spider web and hedgehog spine structures in the failure stages by about 20%.

### 3.2. Strain energy analysis

During the impact process, the energy absorbed by the thin-walled structure is mainly stored in the form of strain energy and the rest of the energy is dissipated as kinetic energy and friction energy. Figure 6 illustrates the strain energy density fields of the five thin-walled structures at the moment before failure. At the moment before failure, the overall strain energy density level in the single-walled cylinder is low, and the annular narrow band on the inner side of the outer wall near the end is the main energy storage region (Fig. 6(a)). The overall strain energy density is slightly increased for both spider web structures. Compared with the single-walled cylinder, the strain energy density distribution is more uniform along the height direction of the structure, and the number of island or sheet-like energy storage areas are increased in both the outer wall and the inner structure of the spider web

structure. Moreover, the multilevel design hardly changes the strain energy density distribution of the outer wall of the spider web structure but makes the strain energy density distribution of its inner structure more uniform (Fig. 6(b) and (c)).

The overall strain energy densities of the two hedgehog spine structures are substantially higher. For the simple hedgehog spine structure, the high strain energy density zones are distributed in a web-like pattern in the middle of the outer wall and intermittently in the internal structure (Fig. 6(d)); the multilevel design results in a more uniform deformation of the multilevel hedgehog spine structure, with the entire outer wall and the internal structure except for the ends in the high strain energy density zone (Fig. 6(e)).

### 3.3. Failure modes

The configuration and first principal stress  $\sigma_1$  evolution of the five thin-walled structures under uniaxial impact are illustrated in Fig. 7. The outer wall is the first part where element failure occurs in all the five structures. The first principal stress within the annular narrow band at the outer end of the outer wall of the single-walled cylinder reaches its maximum when the axial displacement is 2.0 mm. Subsequently, element failure occurs, and vertical and transverse cracks occur at the top of the outer wall in sequence, showing a catastrophic failure mode of top-folding fracture (Fig. 7(a)). When the axial displacements are 2.7 mm and 3.0 mm, respectively, the  $\sigma_1$  within the island region near the outer end

of the outer wall of both spider web structures reaches the maximum. Subsequently, element failure occurs, and vertical and transverse cracks occur at the top of the outer wall in sequence. The simple spider web structure demonstrates a progressive failure mode from the top to the middle (Fig. 7(b)); after the introduction of the sub-circle multilevel design, the multilevel spider web structure demonstrates a failure mode of central fragmentation after vertical cracks generated, accompanied by local expansion or contraction of the outer wall in multiple regions (Fig. 7(c)). When the axial displacements are 10.2 mm and 19.3 mm, respectively, the  $\sigma_1$  within the middle region of the outer wall of the hedgehog and multilevel hedgehog structures reaches the maximum. Element failure, vertical crack and transverse crack occur in sequence. Under impact, the two hedgehog structures undergo an outward bending deformation, presenting a failure mode of expansion and fracture in the middle region of the overall structure (Fig. 7(d) and (e)).

### 3.4. Failure mechanism

The stress distribution of the five thin-walled structures at the moment before failure was counted. The structures were divided into 45 equal parts along the axial direction, and the maximum values of the first principal stresses in each part were counted for the outer wall and the inner structure, respectively (Fig. 8(a)). The stresses in the outer wall of the single-walled cylinder and the two spider web structures were not uniformly distributed along the axial direction, with high

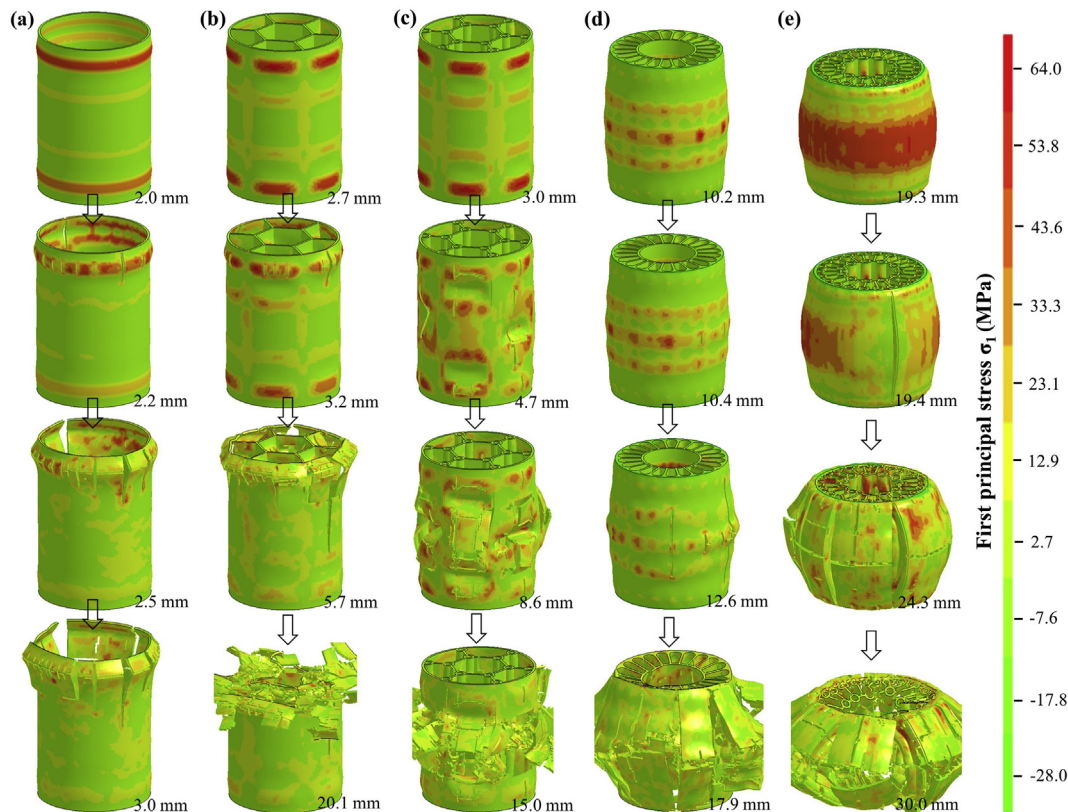
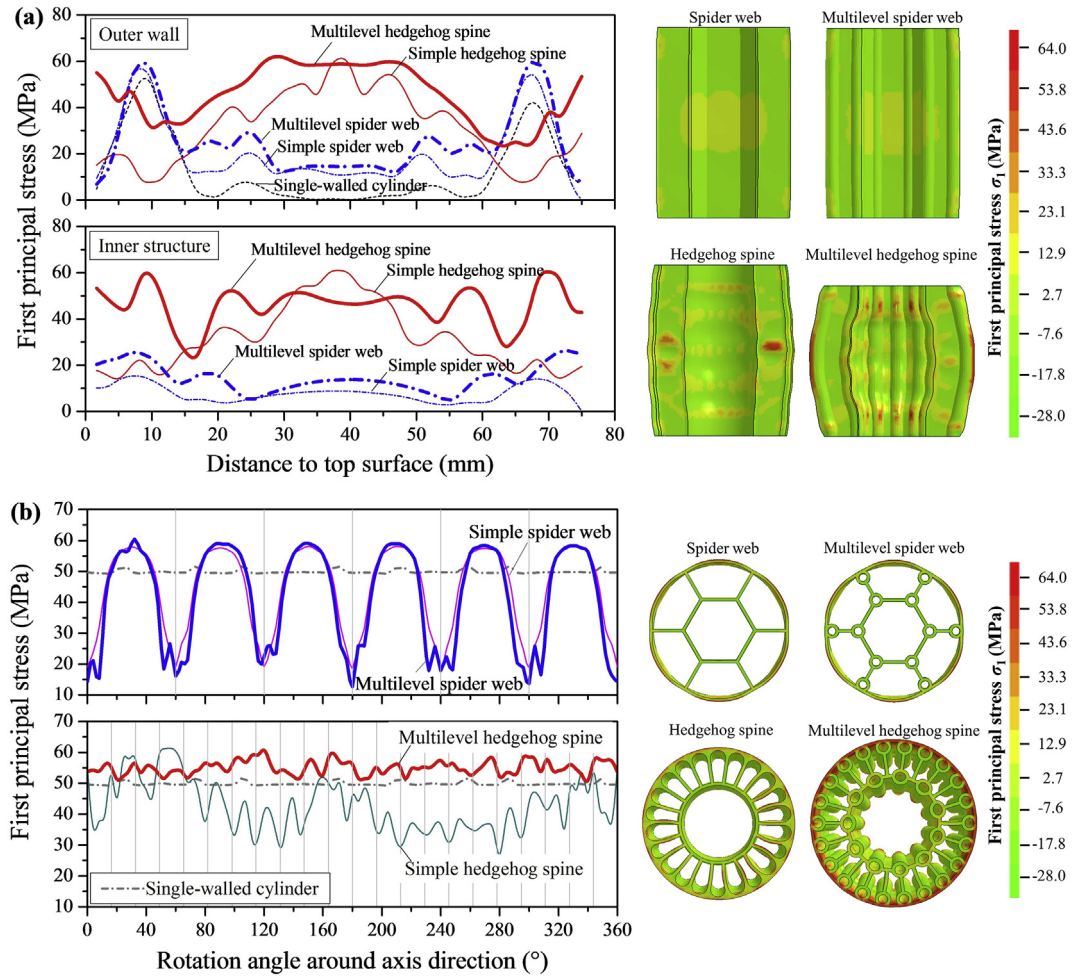


Fig. 7 – Configuration and first principal stress evolution of the five thin-walled structures. (a) Single-walled cylinder; (b) Simple spider web; (c) Multilevel spider web; (d) Simple hedgehog spine; (e) Multilevel hedgehog spine.





**Fig. 8 – Distribution of maximum first principal stress of the five thin-walled structures along the axial direction (a) and the circumferential direction (b) at the moment before failure.**

stresses at the ends and low stresses in the middle. In the middle and near ends of the structure, the stresses were almost zero for the single-walled cylinder and about 12 MPa for the two spider web structures, respectively. The multilevel design further increased the stresses in the near end region by about 10 MPa. The stresses in the outer walls of the two hedgehog spine thin-walled structures were more uniformly distributed, with the stresses in the middle slightly higher than those in the ends. In the middle of the structures, the stresses were significantly increased above 40 MPa. The multilevel design resulted in a more uniform distribution of stresses in the middle, almost all reaching 60 MPa. At the same time, the stresses in the ends were increased, and the overall stresses in the structures were almost at the same level. The stresses in the internal structures of the two spider web structures were more uniformly distributed along the axial direction and were at the same level as that in the outer wall in the middle of the structure. The stresses in the internal structure of the two hedgehog spine structures were more uniformly distributed along the axial direction and were at the same level as that in the outer wall. In other words, the spider web structure and its multilevel structure design failed to share the high stresses at the end of the outer wall of the single-walled cylinder. In

**Table 3 – MIF, SEA, AIF and IFE of the multilevel hedgehog spine structure with different number of ribs and radius of sub-circle before failure.**

Radius of sub-circle (mm)	Number of ribs	MIF (kN)	SEA (kJ/kg)	AIF (kN)	IFE (%)
2.0	6	20.16	1.35	14.23	70.59
2.0	8	23.89	1.54	16.63	69.61
2.0	10	26.67	2.57	20.99	78.70
2.0	12	29.78	4.28	25.26	84.82
2.0	14	33.22	6.82	29.35	88.35
2.0	16	36.37	7.15	31.88	87.65
2.0	18	40.17	9.92	35.70	88.87
2.0	20	43.61	12.92	39.29	90.09
2.0	22	47.20	13.86	42.21	89.43
1.8	22	44.84	12.89	40.32	89.92
1.6	22	42.60	12.02	38.43	90.21
1.4	22	40.50	10.82	36.48	90.07
1.2	22	37.02	6.75	32.83	88.68
1.0	22	36.30	6.66	31.75	87.47
0.8	22	34.55	5.99	30.00	86.83
0.5	22	31.85	4.62	27.00	84.77

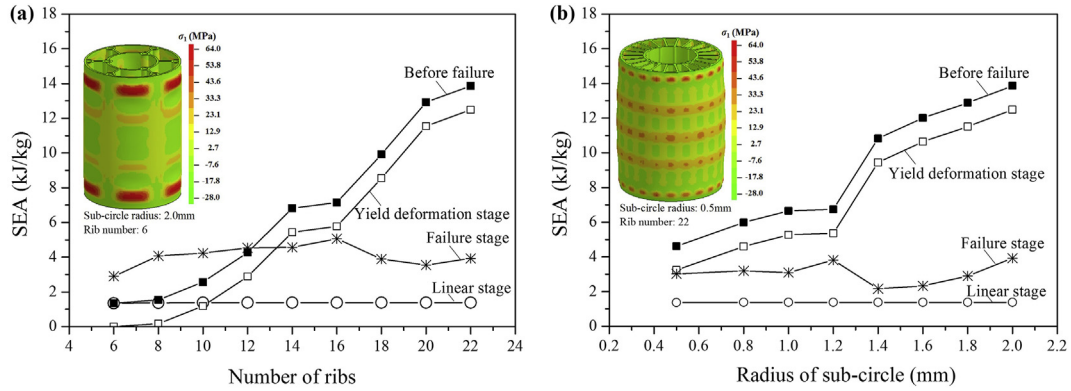


**Fig. 9 – Influence of the number of ribs (a) and the radius of sub-circle (b) on the specific energy absorption of the multilevel hedgehog spine structure.**

contract, the hedgehog spine structure and its multilevel design could distribute the stresses in the thin-walled structure under impact to the whole structure instead of concentrating them in the outer wall.

The structures were divided into 90 equal parts along the circumferential direction, and each part point was connected with the center of the circle to form multiple sectors, with the positive x axis as the 0°. The maximum values of the first principal stresses in all elements in each sector were counted clockwise (Fig. 8(b)). The stresses in the outer and inner walled area connected with ribs of the two spider web structures were largely decreased, while the stresses were much higher between two adjacent ribs. It can be seen that such simple ribs does not make the stress distribution of the inner and outer wall uniform along the circumference, the amplitude of stress fluctuation is about 50 MPa. By comparison, the stresses of the two hedgehog spine structures were more uniformly distributed along the circumferential direction due to the arc design of the joint between the ribs and the outer all and the increase of the number of ribs. The amplitudes of stress fluctuation are within 50 MPa for the simple hedgehog spine structure and only 10 MPa for the multilevel hedgehog spine structure, which much lower than the two spider web structures. That is to say, the multilevel design improves the deformation coordination ability, and the stress distribution along the circumference of the whole structure was further improved and more uniform.

#### 4. Parametric design of multilevel hedgehog spine structure

The MIF, SEA, AIF and IFE of the multilevel hedgehog spine structure with different number of ribs and radius of sub-circle before failure were shown in Table 3. Obviously, as the number of ribs or radius of sub-circle increased, the SEA of the multilevel hedgehog spine structure was gradually improved. Specifically, when the number of ribs was increased from 6 to 22, the SEA of the multilevel hedgehog spine structure with a sub-circle radius of 2.0 mm was increased by 9.3 times. When the sub-circle radius was increased from 0.5 mm to 2.0 mm, the SEA of the multilevel hedgehog spine structure with 22 ribs was

increased by 2.0 times. The MIF and AIF of the multilevel hedgehog spine structure could be increased with the increasing of the number of ribs or radius of sub-circle. In addition, the IFE of the multilevel hedgehog spine structure could be promoted by increasing the number of ribs. When the number of ribs was increased from 6 to 22, the IFE of the multilevel hedgehog spine structure with a sub-circle radius of 2.0 mm was increased from 70.59% to 89.43%. By contrast, increasing the radius of sub-circle had little effect on the IFE of the multilevel hedgehog spine structure with 22 ribs. The multilevel hedgehog spine structure with the smallest radius of sub-circle still had high IFE. For the multilevel hedgehog spine structure, as the number of ribs or the radius of sub-circle increased, the stress distribution along the axial direction and the circumferential direction became more uniform with increasing stress and improved deformation ability in the middle area of structure (Fig. 9(a)), which can effectively improve the SEA in the yield deformation stage while having little effect on the SEA in the linear and failure stages (Fig. 9(b)).

#### 5. Conclusions

Thin-walled structures of simple hedgehog spine and multilevel hedgehog spine structures were designed, inspired by the hedgehog spine's cross section and the beetle forewing's hollow circle substructure, which both have high resistance to impact. Compared with thin-walled structures of conventional single-wall cylinder, the simple and multilevel spider webs with relatively high energy absorption [15], the energy absorption properties in the process of impact compression of the thin-walled structures of the simple hedgehog spine and multilevel hedgehog spine were analyzed and the following conclusions were obtained:

The stresses of the single-walled cylinder and the simple spider web thin-walled structure were not uniformly distributed, with high stresses at the ends and low stresses in the middle so that their overall strain energy density level is low. The hedgehog spine cross section design can effectively improve the deformation coordination ability and stress distribution of the structure, and disperse the stress into the whole structure, which makes the structure have a wide range

of high strain energy density area. The specific energy absorption just before failure of the simple hedgehog spine thin-walled structure is 9.6 times and 5.7 times those of the single-wall cylinder and simple spider web thin-walled structure, respectively.

After the introduction of the sub-circle design, the stress of the multilevel spider web thin-walled structure is still concentrated at the ends, the strain energy distribution of the internal structure is slightly improved, and the specific energy absorption is only about 20% higher than that of the simple spider web thin-walled structure. However, the range of high strain energy density of the multilevel hedgehog spine thin-walled structure gets further increased, and the specific energy absorption is 2.1 times that of the simple hedgehog spine thin-walled structure.

Moreover, increasing the number of ribs or the sub-circle radius of multilevel hedgehog spine thin-walled structure can make the stress distribution of the whole structure more uniform, thus improving the specific energy absorption of the structure.

---

### Declaration of Competing Interest

The authors declare that they have no known competing financial interests or personal relationships that could have appeared to influence the work reported in this paper.

---

### Acknowledgments

The authors gratefully acknowledge the support provided by the National Natural Science Foundation of China (No. 11672297), the Strategic Priority Research Program of the Chinese Academy of Sciences (No. XDB22020200).

---

### REFERENCES

- [1] Ha NS, Lu GX. Thin-walled corrugated structures: a review of crashworthiness designs and energy absorption characteristics. *Thin-Walled Struct* 2020;157:106995.
- [2] Ha NS, Lu GX. A review of recent research on bio-inspired structures and materials for energy absorption applications. *Compos B Eng* 2020;181:107406.
- [3] Marsolek J, Reimerdes HG. Energy absorption of metallic cylindrical shells with induced non-axisymmetric folding patterns. *Int J Impact Eng* 2004;30:1209–23.
- [4] Deb A. Crashworthiness design issues for lightweight vehicles. In: Mallick PK, editor. *Materials, design and manufacturing for lightweight vehicles*; 2021. p. 433–70.
- [5] Bisagni C. Crashworthiness of helicopter subfloor structures. *Int J Impact Eng* 2002;27:1067–82.
- [6] Lazarus BS, Velasco-Hogan A, Gomez-del Rio T, Meyers MA, Jasiuk I. A review of impact resistant biological and bioinspired materials and structures. *J Mater Res Technol* 2020;9:15705–38.
- [7] Miranda P, Pajares A, Meyers MA. Bioinspired composite segmented armour: numerical simulations. *J Mater Res Technol* 2018;8:1274–87.
- [8] Garner SN, Naleway SE, Hosseini MS, Acevedo C, Gludovatz B, Schaible E, et al. The role of collagen in the dermal armor of the boxfish. *J Mater Res Technol* 2020;9:13825–41.
- [9] Song JF, Xu SC, Wang HX, Wu XQ, Zou M. Bionic design and multi-objective optimization for variable wall thickness tube inspired bamboo structures. *Thin-Walled Struct* 2008;125:76–88.
- [10] Liu ST, Tong ZQ, Tang ZL, Liu Y, Zhang ZH. Bionic design modification of non-convex multi-corner thin-walled columns for improving energy absorption through adding bulkheads. *Thin-Walled Struct* 2015;88:70–81.
- [11] Fu J, Liu Q, Liufu K, Deng YC, Fang JG, Li Q. Design of bionic-bamboo thin-walled structures for energy absorption. *Thin-Walled Struct* 2019;135:400–13.
- [12] Huang H, Xu S. Crashworthiness analysis and bionic design of multi-cell tubes under axial and oblique impact loads. *Thin-Walled Struct* 2019;114:106333.
- [13] Weaver JC, Milliron GW, Miserez A, Evans-Lutterodt K, Herrera S, Gallana I, et al. The stomatopod dactyl club: a formidable damage-tolerant biological hammer. *Science* 2012;336:1275–80.
- [14] Amini S, Tadayan M, Idapalapati S, Miserez A. The role of quasi-plasticity in the extreme contact damage tolerance of the stomatopod dactyl club. *Nat Mater* 2015;14:943–50.
- [15] Zhang Y, Wang J, Wang CH, Zeng Y, Chen TT. Crashworthiness of bionic fractal hierarchical structures. *Mater Des* 2018;158:147–59.
- [16] Zhang LW, Bai ZH, Bai FH. Crashworthiness design for bio-inspired multi-cell tubes with quadrilateral, hexagonal and octagonal sections. *Thin-Walled Struct* 2018;122:42–51.
- [17] Zhou M, Huang DQ, Su XL, Zhong JT, Hassanein MF, An L. Analysis of microstructure characteristics and mechanical properties of beetle forewings, *Allomyrina dichotoma*. *Mater Sci Eng* 2020;107:110317.
- [18] Drol CJ, Kennedy EB, Hsiung BK, Swift NB, Tan KT. Bioinspirational understanding of flexural performance in hedgehog spines. *Acta Biomater* 2019;94:553–64.
- [19] Swift NB, Hsiung BK, Kennedy EB, Tan KT. Dynamic impact testing of hedgehog spines using a dual-arm crash pendulum. *J Mech Behav BioMed* 2016;61:271–82.
- [20] Wang J, Zhang Y, He N, Wang CH. Crashworthiness behavior of Koch fractal structures. *Mater Des* 2018;144:229–44.
- [21] Sun GY, Pang T, Fang JG, Li GY, Li Q. Parameterization of criss-cross configurations for multiobjective crashworthiness optimization. *Int J Mech Sci* 2017;124:145–57.
- [22] Wei ZQ, Xu XH. Gradient design of bio-inspired nacre-like composites for improved impact resistance. *Compos B Eng* 2021;215:108830.
- [23] Jia Za Yu Y, Hou SY, Wang LF. Biomimetic architected materials with improved dynamic performance. *J Mech Phys Solid* 2019;125:178–97.
- [24] Kelly PA. *Mechanics lecture notes: an introduction to solid mechanics*. The University of Auckland; 2013. p. 97–100.
- [25] Gu GX, Takaffoli M, Buehler MJ. Hierarchically enhanced impact resistance of bioinspired composites. *Adv Mater* 2017;29:1700060.
- [26] Ls-Dyna®. *Keyword user's manual*, livemore. California, USA: Livemore Software Technology Corporation; 2007.